Vol. 84 No. 3 pp. 597–613 ACTA GEOLOGICA SINICA (English Edition) June 2010

REE and C-O Isotopic Geochemistry of Calcites from the World-class Huize Pb-Zn Deposits, Yunnan, China: Implications for the Ore Genesis

HUANG Zhilong[1, 2, *], LI Xiaobiao[1, 3], ZHOU Meifu[2], LI Wenbo[1, 4] and JIN Zhongguo[1]

1 *State Key Laboratory of Ore Deposit Geochemistry, Institute of Geochemistry, the Chinese Academy of Sciences, Guiyang 550002, China*

2 *Department of Earth Sciences, University of Hong Kong, Hong Kong, China*

3 *Graduate School, the Chinese Academy of Sciences, Beijing 100039, China*

4 *MOE Key Laboratory of Orogenic Belts and Crustal Evolution, Peking University, Beijing 100871, China*

Abstract: The world-class Huize Pb-Zn deposits of Yunnan province, in southwestern China, located in the center of the Sichuan-Yunnan-Guizhou Pb-Zn polymetallic metallogenic province, has Pb+Zn reserves of more than 5 million tons at Pb+Zn grade of higher than 25% and contains abundant associated metals, such as Ag, Ge, Cd, and Ga. The deposits are hosted in the Lower Carboniferous carbonate strata and the Permian Emeishan basalts which distributed in the northern and southwestern parts of the orefield. Calcite is the only gangue mineral in the primary ores of the deposits and can be classified into three types, namely lumpy, patch and vein calcites in accordance with their occurrence. There is not intercalated contact between calcite and ore minerals and among the three types of calcite, indicating that they are the same ore-forming age with different stages and its forming sequence is from lumpy to patch to vein calcites.

This paper presents the rare earth element (REE) and C-O isotopic compositions of calcites in the Huize Pb-Zn deposits. From lumpy to patch to vein calcites, REE contents decrease as LREE/HREE ratios increase. The chondrite-normalized REE patterns of the three types of calcites are characterized by LREE-rich shaped, in which the lumpy calcite shows $(La)_N < (Ce)_N < (Pr)_N \approx (Nd)_N$ with $Eu/Eu^* < 1$, the patch calcite has $(La)_N < (Ce)_N < (Pr)_N \approx (Nd)_N$ with $Eu/Eu^* > 1$, and the vein calcite displays $(La)_N > (Ce)_N > (Pr)_N > (Nd)_N$ with $Eu/Eu^* > 1$. The REE geochemistry of the three types of calcite is different from those of the strata of various age and Permian Emeishan basalt exposed in the orefield. The $\delta^{13}C_{PDB}$ and $\delta^{18}O_{SMOW}$ values of the three types of calcites vary from −3.5‰ to −2.1‰ and 16.7‰ to 18.6‰, respectively, falling within a small field between primary mantle and marine carbonate in the $\delta^{13}C_{PDB}$ vs $\delta^{18}O_{SMOW}$ diagram.

Various lines of evidence demonstrate that the three types of calcites in the deposits are produced from the same source with different stages. The ore-forming fluids of the deposits resulted from crustal-mantle mixing processes, in which the mantle-derived fluid components might be formed from degassing of mantle or/and magmatism of the Permian Emeishan basalts, and the crustal fluid was mainly provided by carbonate strata in the orefield. The ore-forming fluids in the deposits were homogenized before mineralization, and the ore-forming environment varied from relatively reducing to oxidizing.

Key words: gangue calcite, REE geochemistry, C-O isotope, ore-forming fluid, Huize Pb-Zn deposits

1 Introduction

In SW China, more than 400 Pb-Zn ore deposits or mineralizations comprise the well-known Sichuan-Yunnan-Guizhou Pb-Zn polymetallic metallogenic province (Liu and Lin, 1999). Most of these ore deposits or mineralizations are spatially associated with Permian Emeishan basalts aged c.260 Ma (Boven et al., 2002; Lo et al., 2002; Zhou et al., 2002; Ali et al., 2004; Fan et al., 2008) and are controlled by fault zones (Fig. 1). The relationship between Emeishan basalts and Pb-Zn

* Corresponding author. E-mail: huangzhilong@vip.gyig.ac.cn

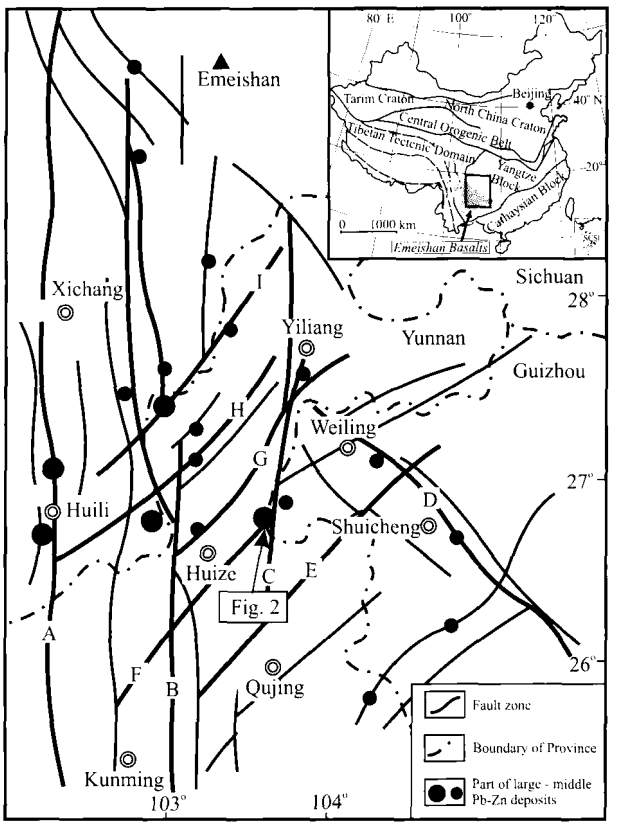

Fig. 1. Tectonic map of the the Sichuan-Yunnan-Guizhou Pb-Zn polymetallic metallogenic province and distribution of part of the large-middle Zn-Pb deposits (taken from Han et al., 2007; brief revising).

Major NS-trending tectonic zones: (A) the Xichang-Yimen fault zone, (B) the Xiaojiang fault zone, (C) the Zhaotong-Qujing fault zone. Major NW-trending tectonic zone: (D) the Weining-Shuicheng fault zone. Major NE-trending tectonic zones: (E) the Xundian-Xuanwei fault zone, (F) the Dongchuan-Zhenxiong fault zone, (G) the Huize-Yiliang fault zone, (H) the Ludian-Yanjin fault zone, (I) the Yongshan-Suijiang fault zone.

mineralization in this district was examined by numerous works (Zhang et al., 1988; Liu and Lin, 1999; Huang et al., 2001, 2004a,b; Hu et al., 2005). The world-class Huize Pb-Zn deposit, Yunnan Province, located in the center of the Sichuan-Yunnan-Guizhou Pb-Zn polymetallic metallogenic province (Fig. 1), has Pb+Zn reserves of more than 5 million tons at a Pb+Zn grade of higher than 25%, and contains abundant associated metals, such as Ag, Ge, Cd, and Ga. The geology of these deposits (Zhou et al., 2001; Han et al., 2007), ore-controlling structures (Han et al, 2000, 2007), ore-forming ages (Huang et al., 2001; Li et al., 2007a), and the source of the ore-forming metals and fluids (Liu and Lin,1999; Zhou et al., 2001; Han et al., 2004; Li et al., 2006) have been investigated widely. However, there is still a matter of debate about the source of ore-forming metals and ore-forming fluids of these deposits (Liu and Lin, 1999; Zhou et al., 2001; Huang et al., 2004a; Han et al., 2004; Li et al., 2006).

Calcite is a common gangue mineral in many deposits and has been used for constraint the source and evolution of ore-forming fluids (Zheng and Chen, 2003). Because the $\delta^{13}C_{PDB}$ and $\delta^{18}O_{SMOW}$ values of many mantle-derived carbonatites are outside the range of the $\delta^{13}C_{PDB}$ (from −4‰ to −8‰) and $\delta^{18}O_{SMOW}$ values (from 6‰ to 10‰) for primary mantle (PM) (Taylor et al., 1967; Demény et al., 1998), the use of C-O isotopes to constrain the source and evolution of ore-forming fluids often enable various explanations. In the last two decades, rare earth element (REE) geochemistry of hydrothermal minerals, especially Ca-minerals, such as fluorite, calcite, apatite and scheelite have been used to trace the origin of ore deposits (Lottermoser, 1992 and references therein; Subias and Fernandez-Nieto, 1995; Whitney and Olmsted, 1998; Hecht et al., 1999; Ghaderi et al., 1999; Brugger et al., 2000; Monecke et al., 2000; Bau et al., 2003; Bühn et al., 2003; Alvin et al., 2004; Schwinn and Markl, 2005; Li et al., 2007a; Huang et al., 2007). Calcite is the only gangue mineral in the primary ores from the Huize Pb-Zn deposits. Han et al. (2000) and Li et al. (2007a) suggested that REE in the primary ores from these deposits are mostly hosted in gangue calcite. Therefore, study on the REE geochemistry of calcite can provide important information about the source and evolution of ore-forming fluids.

Based on REE and C-O isotopic compositions of calcite from the Huize Pb-Zn deposits, in combination with other geological and geochemical data, the source and evolution of ore-forming fluids, and the relationship between Emeishan basalts and Pb-Zn mineralization are discussed in this paper.

2 Geologic Setting

The Huize Pb-Zn deposits are located in the intersection of the NE-trending secondary fault zone of the Xiaojiang fault zone, the NS-trending Zhaotong-Qujing fault zone and the NW-trending Weining-Shuicheng tectonic zone (Fig. 1). The surface geology and a representative section of the stratigraphy are shown in Figs 2 and Fig. 3, respectively. The deposits are hosted in the Lower Carboniferous carbonate strata (Baizuo Formation; Fig. 3) and fault-controlled. The structures are mainly the north-east fault including Kuangshanchang, Qilinchang, Yinchangpo and Niulanjiang faults (Fig. 2). These faults are characterized by multi-episodic activities and are related to the Pb-Zn mineralization (Han et al., 2000, 2007). The Permian Emeishan basalts, whose age is c.260 Ma (Boven et al., 2002; Lo et al., 2002; Zhou et al., 2002; Ali et al., 2004; Fan et al., 2008) are exposed in the northern and southwestern parts of the orefield (Fig. 2).

The Huize Pb-Zn deposits are composed of the Kuangshanchang and Qilinchang ore deposit (Fig. 2).

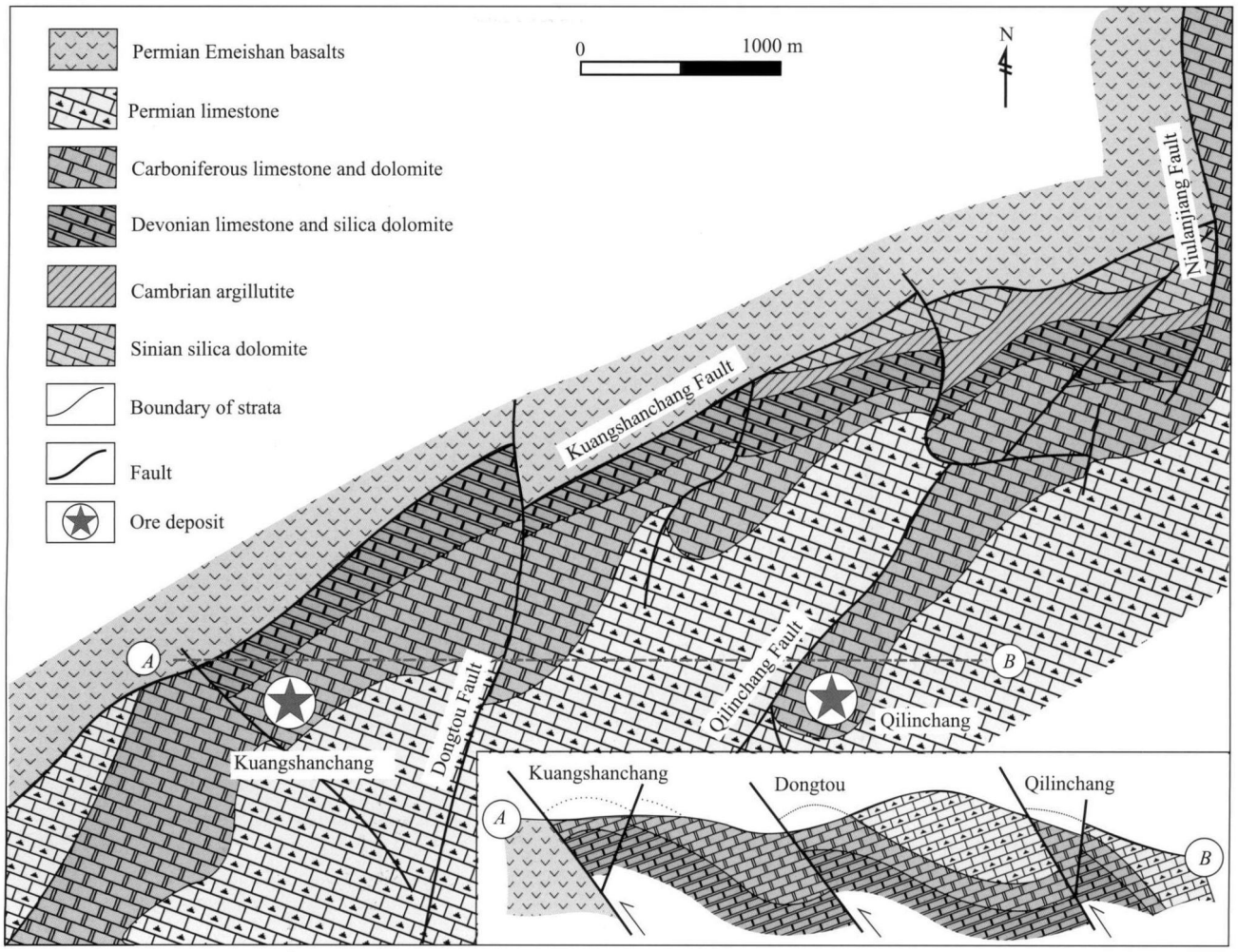

Fig. 2. Geological map of the Huize Pb-Zn deposits (modified from Han et al., 2007)

Zhou et al. (2001) and Han et al. (2007) described the geological setting and characteristics of the deposits. In recent years, four primary orebodies whose Pb+Zn reserves vary from 0.5 million tons to 1 million tons were found in the depths of these deposits. Orebody No. 6, No. 8 and No. 10 are in depth of Qilinchang, the outcrop level of which is 1631 m, 1571 m and 1471 m, respectively, and orebody no. 1 is in depth of Kuangshanchang the outcrop level of which is 1751 m. With the exception of weak oxidation of parts of orebody no. 1, the four orebodies are similar in mineral associations and contain galena, sphalerite and pyrite as ore minerals, and calcite as gangue mineral. The characteristics of the deposits are summarized as follows. (1) The carbonate strata of various ages are exposed in the orefield (Fig. 2 and Fig. 3), but only the Lower Carboniferous Baizuo Formation is the ore-hosting stratum. (2) The distinct boundaries between ore bodies and host rocks (Fig. 4a, b, c), and the wall-rock alteration of dolomitization, pyritization and limonitization were observed (Fig. 4d). (3) The Pb+Zn grade in orebodies is extremely high, such as the average Pb+Zn grade of orebody no. 6, no. 8, no. 10 and no. 1 can reach up to 34.6%, 25.8%, 33.5% and 32.6%, respectively, and orebodies contain an abundance of accompanying elements, including Ag, Ge, Cd, and Ga. (4) From the bottom to the top of the primary orebody, the mineral assemblages exhibit differentiation from coarse pyrite + ferrous sphalerite + calcite to sphalerite + galena + pyrite + calcite to fine pyrite + calcite.

Calcite is the only gangue mineral in the primary ores from the Huize Pb-Zn deposits and can be classified into three types, namely lumpy, patch and vein calcites in accordance with their occurrence (Fig. 5a). The lumpy calcite is irregular in shape, usually more than 10 cm × 10 cm × 10 cm in size, with sharp boundaries with the ore minerals (Fig. 5b). The patch calcite is evenly scattered within the ore minerals, mostly less than 5 cm × 5 cm × 5 cm in size, showing no distinct boundaries with the ore minerals (Fig. 5b). The vein calcite occurs as veins penetrating the ore minerals, generally less than 2 cm in width and within the range of 5 cm to 20 cm in length, showing distinct boundaries with the ore minerals (Fig.

Age	Name	Column	Thickness (m)	Lithologic Characteristics
Permian	Emeishan basalts		600–800	Grey-brown massive, amygdaloidal and vesiculate basalts, in middle-above occurrs purple vein or lenticullar altered basalts and accidental see lameller copper, discordant contact with the below strata.
	Qixia-Maokou Formation		450–600	Dark-grey, grey and light-grey limestone, dolomitic limestone mix up dolomite, the dolomitic matter occurr as massive and tiger-spot in limestone, conformable contact with the below strata.
	Liangshan Formation		20–60	The above is the interbeds of grey-blue carbonaceous shale and quartz sandstone, the below is quartz sandstoe mix up yellow-brown argillutite, conformable contact with the below strata.
Carboni-ferous	Maping Formation		20–90	Purple and grey-purple syngenetic pebble limestone, the middle mix up purple-red and yellow-green shale, the top is pisolitic limestone, conformable contact with the below strata.
	Weining Formation		10–20	Light-grey limestone mix up oolitic limestone, the bottom is dolomitic limestone, conformable contact with the below strata.
	Baizuo Formation		40–60	Grey-white, cream-coloured and flesg-red coarse dolomite mix up light-grey limestone and dolomitic limestone, the most important ore-hosting stratum, the Pb-Zn ore bodies host in the light coase dolomite, conformable contact with the below strata.
	Datang Formation		5–30	Grey cryptocrystal limestone and oolitic limestone, the top is grey-brown siltstone and purple mudstone, disconformable contact with the below strata.
Devonian	Zaige Formation		100–310	The above is grey cryptocrystal limestone and yellow-white mid-crystal dolomite, the middle is mid-thick bedded powdered crytsal siliceous dolomite, the below is light-grey mid-thick fine-mid crystalline dolomite mix up light-grey pelitic dolomite, dis-conformable contact with the below strata.
	Haikou Formation		0–15	The interbeds of light-yellow sandstone or siltstone and green, grey-black argillutite. disconformable contact with the below strata.
Cambrian	Qongzhusi Formation		0–70	Black argillutite mix up yellow sandy mudstone, disconformable contact with the below strata.
Sinian	Dengying Formation		> 70	Grey-white siliceous dolomite, fault contact with the below strata.

The Liangshan Formation and Haikou Formation do not outcrop in Fig.2.

Fig. 3. Histogram of the strata of the Huize Pb-Zn deposits

5d). As for their respective quantities, the three types of calcites follow the descending order of lumpy calcite> patch calcite> vein calcite. On the basis of the contact relations with the ore minerals, in combination with minerographical observations (Huang et al., 2004b), three types of calcites are the same ore-forming age but at different stages and its forming sequence is from lumpy to patch to vein calcites.

3 Sample Preparation and Analytical Methods

Three types of calcites were collected from orebodies no. 1, no. 6, no. 8 and no. 10 of the Huize Pb-Zn deposits.

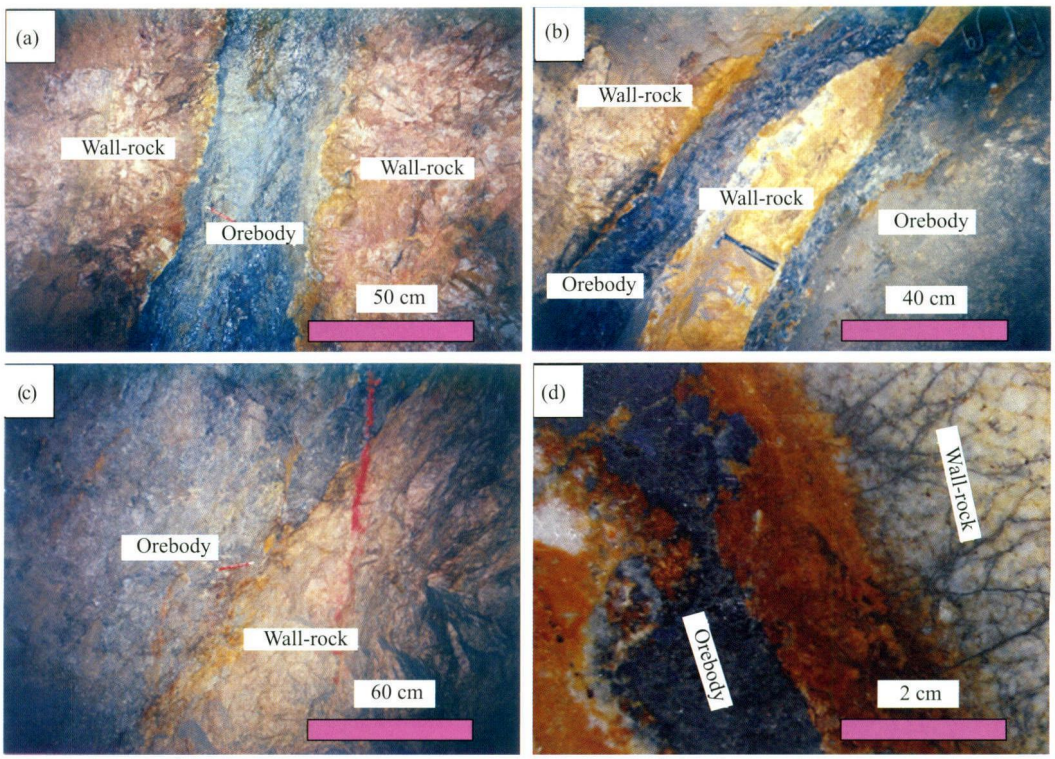

Fig. 4.Contact relationship between orebody and host rock of the Huize Pb-Zn deposits.
(a), (b) and (c) Photographs showing the distinctive boundary in orebody no.6, displaying the distinctive boundary between the orebody and the wall-rock (the Lower Carboniferous Baizuo Formation). (d) Photograph of the drilling core from Orebody no.8 showing simple dolomitization and limonitization between the orebody and the wall-rock (the Lower Carboniferous Baizuo Formation).

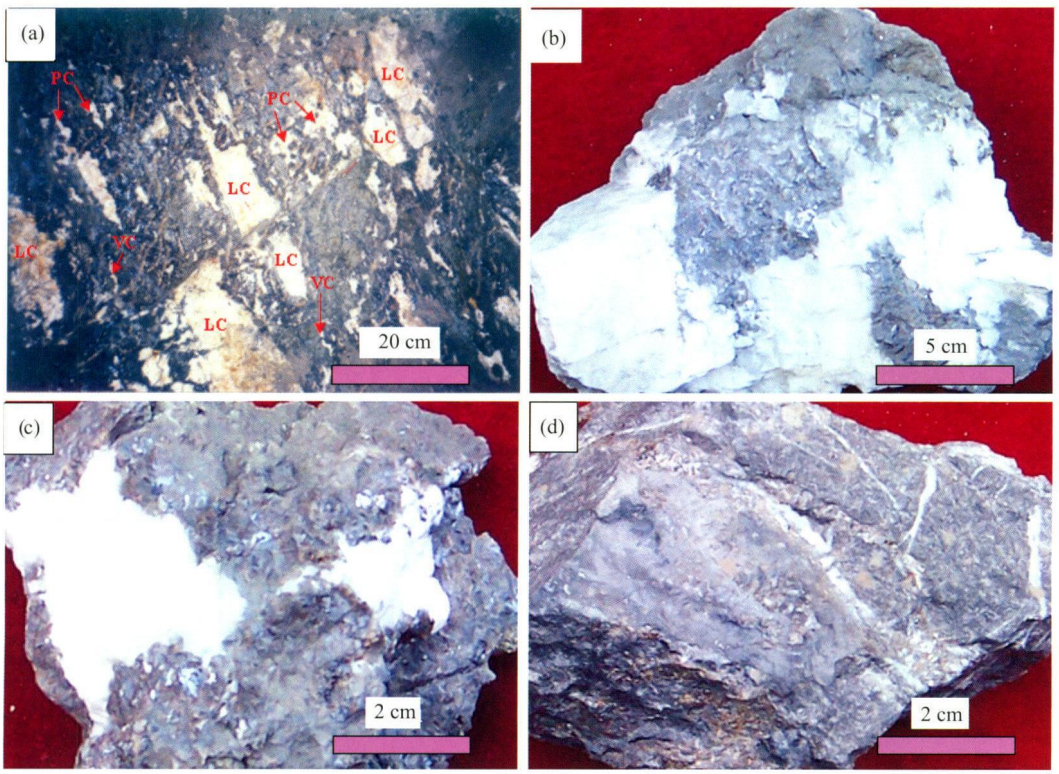

Fig. 5. Photographs showing the gangue calcite in primary ores from the Huize Pb-Zn depsoits.
(a) The distribution of the ore mineral (black, is mainly comprised of galena, sphalerite and pyrite) and gangue mineral (LC, lumpy calcite; PC, patch calcite; VC, vein calcite) in orebody no. 6; (b) the lumpy calcite in primary ores from orebody no. 10; (c) the patch calcite in primary ores from orebody no. 6, and (d) the vein calcite in primary ores from orebody no. 1.

Selected calcite grains were analyzed for major elements, REE contents and C-O isotopic compositions. For comparison, the ore-hosting stratum (the Baizuo Formation) and drusy calcite of carbonate strata in the orefield were measured for major elements, REE contents and C-O isotopes. REE contents of the strata of various age and the Emeishan basalts in the orefield were also determined.

Because calcite is the only gangue mineral in the primary ores from the Giant Huize Pb-Zn deposits, samples of lumpy, patch and vein calcites were easy to select. Lumpy calcite was directly sampled from the primary orebodies. After being lightly crushed, pure calcite was picked out. The methods of selecting patch and vein were the same. The specimens of the patch and vein calcite were crushed to 40–60 mesh in grain size, and then calcite was separated from ores using heavy liquid. After being washed in alcohol and dried, the patch or vein calcites were picked out under a binocular microscope. The selected samples of lumpy, patch and vein calcites were cleaned in distilled water and dried again, and finally, ground to less than 200 mesh in grain size for analysis.

Major elements of whole-rock samples were determined by wet chemical methods at the Institute of Geochemistry, the Chinese Academy of Sciences. REE contents were analyzed in solution by inductively coupled plasma mass spectrometry (ICP-MS) at the Institute of Geochemistry, the Chinese Academy of Sciences. The analytical procedure was conducted by Qi et al. (2000). Fifty milligrams of whole-rock powder were dissolved in a Teflon bomb using 1 mL HF and 0.5 mL HNO_3. The sealed bomb was placed in an electric oven and heated to 190°C for 12 h. One milliliter of 1 u g mL^{-1} Rh was added to the cooled solution as the internal standard and the solution was then evaporated. One milliliter of HNO_3 was added, evaporated to dryness and followed by a second addition of HNO_3 and evaporation to dryness. The final residue was re-dissolved in 8 mL HNO_3. The bomb was sealed and heated in an electric oven at 110°C for 3 h. The final solution was diluted to 100 mL by the addition of distilled de-ionized water for ICP-MS analysis. The analytical precision is better than 10%.

The C-O isotopes were analyzed at the Isotopic Laboratory of the Institute of Mineral Resources, Chinese Academy of Geological Sciences. The analytical method was the 100% phosphorate method (McCrea, 1950). After the release of CO_2 by the reaction between calcite and phosphoric acid at 25°C, the $\delta^{13}C_{PDB}$ and $\delta^{18}O_{PDB}$ values of calcite was directly measured from CO_2 by MAT-251 EM, with an analytical precision of ±0.2‰. The formula of Friedman and O'Neil (1977), $\delta^{18}O_{SMOW}$=1.03086 $\delta^{18}O_{PDB}$+30.86, was used to transform $\delta^{18}O_{PDB}$ into $\delta^{18}O_{SMOW}$.

4 Results

The major elements, REE contents and C-O isotopes of the three types of calcites as well as the Baizuo Formation and drusy calcite in carbonate strata are listed in Table 1 and Table 2, respectively. Table 3 presents the statistical results of REE contents of calcite, strata of various ages and the Emeishan basalts in the orefield.

4.1 Major Elements

There is no significant difference in SiO_2, Al_2O_3, CaO, Na_2O and CO_2 contents of lumpy, patch and vein calcites in the deposits with the exception of Sample Cal-3 and Cal-5, which have higher Fe_2O_3, FeO, MnO and MgO and lower Na_2O than those of the other samples (Table 1). Fe_2O_3, FeO, MnO and MgO contents in the lumpy, patch and vein calcites are higher than those of drusy calcite in carbonate strata, and the CaO/(Fe_2O_3+FeO+MnO+MgO+CaO) ratios of the former (from 94.55% to 97.63%) are lower than those of the latter (from 98.98% to 99.13%). Fig. 6 shows that lumpy, patch and vein calcites fall within the field relatively near (Fe_2O_3+FeO+MnO) end and drusy calcite near CaO end .

Rare earth elements From Tables 1 and 3, some differences of REE geochemical features among the three types of calcites in the Huize deposits were observed. From lumpy to patch to vein calcites, the REE (including Y) contents decreased from 31.90–357.14 μg/g to 22.60–106.67 μg/g to 23.70–36.24 μg/g, as LREE/HREE ratios increase (from 3.73–17.91 to 8.22–24.95 to 30.71–40.70). The chondrite-normalized REE patterns of the three types of calcites are LREE-rich shaped, in which the lumpy calcite shows $(La)_N < (Ce)_N < (Pr)_N \approx (Nd)_N$ with $Eu/Eu^* < 1$ (0.33–0.96), the patch calcite is characterized by $(La)_N < (Ce)_N < (Pr)_N \approx (Nd)_N$ with $Eu/Eu^* > 1$ (1.1–2.04), and the vein calcite displays $(La)_N > (Ce)_N > (Pr)_N > (Nd)_N$ with $Eu/Eu^* > 1$ (1.73–2.53) (Fig. 7). Their $(La/Sm)_N$, $(La/Pr)_N$, $(Gd/Yb)_N$, and $(La/Yb)_N$ have obvious differences among the three types of calcites (Table 1 and Table 3).

The REE geochemistry of the three types of calcite in the deposits is different from that of drusy calcite of carbonate strata. REE contents of the former are much higher than that of the latter (Table 1). With the exception of Sample HZQ-35 (ΣREE is 9.74 μg/g), ΣREE of drusy calcite is less than 3 μg/g. Because the contents of most of the REEs in drusy calcite are below the detection limit, their chondrite-normalized REE patterns are irregular (diagram omitted) and the Eu/Eu^* and Ce/Ce^* values have a wide range (from 0.74 to 3.71 and 0.61 to 1.18,

Table 1 The major elements (wt%) and rare earth elements (REE) (μg/g) of calcites from the Huize giant Pb-Zn deposits

Occurrence						Lumpy calcite										
Sample no.	HZ-911-8	HZ-911-10	HZ-911-12	HZ-911-15	HZ-911-37	HZQ-25	HZQ-27	HZQ-47	HZQ-61	HZQ-66	HZQ-80	HZQ-96	HZQ-100	HZQ-101	Cal-1	Cal-3
SiO_2		3.30	3.15			2.20							1.78		2.30	2.02
TiO_2		0.17	0.19			0.05							0.02		0.07	0.20
Al_2O_3		0.09	0.10			0.11							0.14		0.05	0.19
Fe_2O_3		0.30	0.39			0.40							0.59		1.20	0.95
FeO		0.14	0.20			0.21							0.29		0.20	0.25
MnO		0.54	0.54			0.43							0.59		0.78	0.79
MgO		0.40	0.61			0.41							0.42		1.00	0.90
CaO		55.17	55.15			55.10							55.20		55.15	55.00
Na_2O		0.33	0.34			0.33							0.35		0.10	0.11
K_2O		0.13	0.15			0.17							0.36		0.01	0.01
LOI		0.70	0.65			0.40							0.40		0.50	0.25
P_2O_5		0.18	0.13			0.10							0.10		0.07	0.10
CO_2		38.05	38.15			39.80							39.60		38.05	39.10
Total		99.50	99.75			99.71							99.84		99.48	99.87
La	2.49	3.36	5.41	15.82	6.59	7.35	2.73	13.91	4.93	3.15	6.55	4.38	3.91	2.03	13.51	18.30
Ce	10.42	14.26	20.05	51.15	22.63	32.39	11.54	58.09	21.56	10.07	29.35	20.53	20.75	9.28	62.12	91.06
Pr	1.70	2.42	3.18	7.46	3.46	5.90	2.16	10.65	3.75	1.61	5.51	3.65	4.46	1.84	11.43	16.98
Nd	8.44	11.72	12.97	29.09	14.83	29.18	10.35	52.20	20.98	7.45	28.46	19.44	25.91	10.47	54.31	85.50
Sm	2.36	2.90	2.50	5.16	2.46	6.18	2.08	11.51	4.72	1.48	5.88	4.56	6.91	2.79	14.52	23.05
Eu	0.38	0.41	0.36	0.68	0.48	1.14	0.46	2.03	0.76	0.36	0.88	1.29	1.54	0.63	1.45	3.51
Gd	2.17	2.79	2.06	3.98	1.96	4.94	1.98	10.46	3.95	1.28	4.84	3.73	6.20	2.30	12.78	20.62
Tb	0.37	0.37	0.20	0.34	0.19	0.50	0.17	1.23	0.46	0.16	0.43	0.38	0.82	0.25	1.46	2.44
Dy	2.09	2.13	0.69	1.25	0.66	2.31	0.81	6.39	2.22	0.76	1.75	1.70	4.41	1.12	6.72	11.16
Ho	0.37	0.38	0.12	0.15	0.09	0.34	0.12	0.99	0.32	0.11	0.26	0.25	0.65	0.17	0.98	1.58
Er	1.08	1.06	0.17	0.29	0.21	0.66	0.22	2.30	0.67	0.24	0.53	0.53	1.36	0.31	2.03	3.20
Tm	0.13	0.13	0.02	0.02	0.01	0.05	0.03	0.24	0.05	0.02	0.04	0.05	0.13	0.03	0.16	0.27
Yb	0.66	0.79	0.04	0.08	0.09	0.20	0.11	1.14	0.21	0.06	0.22	0.34	0.56	0.15	0.71	1.09
Lu	0.07	0.10	0.01	0.01	0.01	0.02	0.01	0.12	0.02	n.d.	0.02	0.04	0.06	0.02	0.07	0.10
Y	14.09	17.15	5.19	8.70	4.77	15.12	5.66	42.29	14.66	5.17	12.86	11.14	28.03	8.03	48.36	78.30
∑REE	46.81	59.95	52.96	124.16	58.44	106.28	38.43	213.56	79.25	31.90	97.57	72.03	105.68	39.40	230.60	357.14
∑LREE	25.80	35.07	44.48	109.35	50.45	82.15	29.32	148.39	56.70	24.11	76.62	53.86	63.47	27.03	157.33	238.39
∑HREE	6.92	7.73	3.30	6.11	3.22	9.02	3.45	22.88	7.89	2.62	8.09	7.02	14.18	4.35	24.91	40.45
LREE/HREE	3.73	4.54	13.50	17.91	15.69	9.11	8.49	6.49	7.18	9.20	9.47	7.68	4.48	6.22	6.32	5.89
Eu/Eu*	0.52	0.45	0.48	0.46	0.67	0.63	0.70	0.57	0.54	0.79	0.51	0.96	0.72	0.76	0.33	0.49
Ce/Ce*	1.22	1.20	1.16	1.13	1.14	1.18	1.14	1.15	1.21	1.08	1.18	1.24	1.20	1.16	1.20	1.24
$(La/Sm)_N$	0.67	0.73	1.36	1.93	1.69	0.75	0.83	0.76	0.66	1.34	0.70	0.61	0.36	0.46	0.59	0.50
$(Gd/Yb)_N$	2.67	2.85	44.84	39.60	17.39	19.74	15.07	7.39	15.49	17.18	18.17	8.81	8.88	12.81	14.58	15.33
$(La/Yb)_N$	2.56	2.87	98.65	131.63	48.85	24.54	17.35	8.21	16.15	35.34	20.52	8.64	4.68	9.43	12.88	11.37
$(La/Pr)_N$	0.58	0.55	0.67	0.84	0.75	0.49	0.50	0.51	0.52	0.77	0.47	0.47	0.35	0.43	0.47	0.42

** The REE contents of drusy calcite of carbonate strata are for reference only. HREE, …; LREE, …; n.d., not detected.

Table 1 Continued

Occurrence	Lumpy calcite		Patch calcite							Vein calcite			Drusy calcite of carbonate strata**			
Sample no.	1571-2	1631(38m)	HZQ-40	HZQ-70	HQ-84	HZQ-85	HZQ-90	HZQ-89-1	HZQ-89-2	HZQ-55	HZQ-77	HZQ-108	HZQ-35	HZK-33	99-18-6	HZ-911-3
SiO_2			2.07					2.09	1.89		2.57				3.56	3.57
TiO_2			0.06					0.17	0.18		0.07				0.04	0.06
Al_2O_3			0.14					0.15	0.10		0.09				0.14	0.10
Fe_2O_3			0.30					0.41	0.50		0.43				0.10	0.12
FeO			0.10					0.20	0.20		0.17				0.06	0.08
MnO			0.55					0.65	0.57		0.59				0.01	0.01
MgO			0.39					0.47	0.38		0.48				0.40	0.27
CaO			55.20					55.25	55.10		55.05				55.15	55.10
Na_2O			0.32					0.48	0.43		0.26				0.33	0.33
K_2O			0.13					0.12	0.15		0.12				0.02	0.18
LOI			0.55					0.35	0.50		0.80				0.45	0.60
P_2O_5			0.01					0.14	0.13		0.05				0.17	0.05
CO_2			39.70					39.50	39.55		39.10				39.50	39.20
Total			99.52					99.98	99.68		99.78				99.93	99.66
La	8.34	7.22	2.27	10.27	17.52	4.50	5.52	4.21	4.27	7.85	6.84	4.68	0.98	0.28	0.29	0.43
Ce	39.84	30.96	7.73	31.62	45.96	16.66	26.74	15.57	21.76	16.07	14.75	10.56	1.04	0.29	0.48	0.91
Pr	7.31	4.92	1.24	4.54	5.70	2.88	4.77	2.63	3.91	1.89	1.80	1.31	0.17	0.04	0.05	0.08
Nd	33.98	22.90	5.71	18.23	21.78	13.96	24.77	12.31	20.66	7.34	7.07	4.91	0.51	n.d.	n.d.	n.d.
Sm	7.23	4.22	1.00	2.40	3.14	2.59	4.73	1.94	4.56	0.79	1.00	0.63	0.17	0.03	0.04	0.09
Eu	1.56	1.13	0.44	1.14	1.82	1.13	1.64	0.99	1.47	0.52	0.49	0.44	0.06	0.01	0.04	0.11
Gd	5.63	3.55	0.79	1.92	2.37	1.97	3.65	1.32	3.40	0.63	0.74	0.45	0.34	0.07	0.06	0.09
Tb	0.47	0.41	0.07	0.13	0.18	0.17	0.37	0.09	0.36	0.04	0.05	0.02	0.05	0.01	0.01	0.01
Dy	1.57	2.21	0.34	0.48	0.81	0.64	1.84	0.34	1.72	0.11	0.16	0.06	0.36	0.08	0.07	0.06
Ho	0.16	0.34	0.06	0.06	0.16	0.09	0.33	0.03	0.26	0.02	0.02	0.01	0.09	0.02	0.01	0.02
Er	0.26	0.89	0.20	0.10	0.52	0.18	0.84	0.09	0.60	0.03	0.04	0.03	0.27	0.04	0.03	0.05
Tm	0.01	0.09	0.04	0.01	0.10	0.02	0.09	0.01	0.08	0.01	0.01	n.d.	0.03	0.01	0.01	0.01
Yb	0.07	0.48	0.18	0.03	0.56	0.11	0.54	0.08	0.42	0.02	0.03	0.02	0.15	0.03	0.03	0.05
Lu	n.d.	0.06	0.03	n.d.	0.11	0.02	0.06	0.01	0.06	n.d.	n.d.	n.d.	0.02	0.01	0.01	0.01
Y	11.48	13.39	2.51	3.37	5.94	4.39	11.32	2.09	10.80	0.92	1.13	0.57	5.49	1.22	0.77	0.89
∑REE	117.91	92.77	22.60	74.31	106.67	49.29	87.20	41.72	74.32	36.24	34.10	23.70	9.74	2.13	1.90	2.81
∑LREE	98.26	71.35	18.39	68.21	95.92	41.71	68.16	37.66	56.63	34.48	31.94	22.53	2.93	0.66	0.91	1.63
∑HREE	8.17	8.03	1.71	2.73	4.81	3.19	7.72	1.97	6.89	0.85	1.04	0.60	1.32	0.25	0.22	0.29
LREE/HREE	12.03	8.89	10.79	24.95	19.94	13.08	8.83	19.09	8.22	40.70	30.71	37.30	2.22	2.60	4.09	5.67
Eu/Eu*	0.75	0.89	1.53	1.63	2.04	1.52	1.21	1.88	1.14	2.25	1.73	2.53	0.74	1.02	2.26	3.71
Ce/Ce*	1.23	1.25	1.11	1.11	1.11	1.12	1.25	1.13	1.28	1.00	1.01	1.03	0.61	0.65	0.95	1.18
$(La/Sm)_N$	0.73	1.08	1.43	2.70	3.51	1.09	0.73	1.36	0.59	6.24	4.32	4.64	3.67	7.10	4.29	2.93
$(Gd/Yb)_N$	64.90	5.97	3.50	50.08	3.42	14.75	5.49	13.19	6.53	34.11	18.00	15.75	1.84	1.77	1.53	1.60
$(La/Yb)_N$	80.33	10.14	8.44	223.44	21.09	28.07	6.92	35.08	6.86	353.01	139.80	137.10	4.38	5.94	6.81	6.29
$(La/Pr)_N$	0.45	0.58	0.72	0.89	1.21	0.62	0.46	0.63	0.43	1.63	1.50	1.41	2.22	2.64	2.26	2.11

Table 2 The C and O isotope of calcite and Baizuo Formation from the Huize giant Pb-Zn deposits

Sample no.	Orebody	Mineral	Occurrence	$\delta^{13}C_{PDB}$	$\delta^{18}O_{SMOW}$
HZ-911-3		Calcite	Patch	−2.2	17.5
HZ-911-10	No.1	Calcite	Lumpy	−3.4	18.4
HZ-911-15		Calcite	Lumpy	−3.5	18.6
HZQ-25		Calcite	Lumpy	−2.5	17.5
HZQ-40		Calcite	Patch	−2.6	17.7
HZQ-47		Calcite	Lumpy	−3.1	17.5
HZQ-55	No.6	Calcite	Vein	−2.7	17.7
HZQ-66		Calcite	Lumpy	−3.4	18.1
HZQ-70		Calcite	Patch	−3.3	18.1
HZQ-77		Calcite	Vein	−2.8	17.8
HZQ-85		Calcite	Patch	−2.7	17.3
HZQ-90		Calcite	Patch	−2.7	17.2
HZQ-96		Calcite	Lumpy	−2.1	17.5
HQ-10-7		Calcite	Lumpy	−2.9	17.0
HQ-10-12		Calcite	Lumpy	−3.2	18.5
HQ-10-18	No.10	Calcite	Lumpy	−2.3	16.8
HQ-10-25		Calcite	Patch	−3.0	17.9
HQ-10-5		Calcite	Vein	−2.8	17.2
HQ-8-115		Calcite	Lumpy	−2.2	17.0
HQ-8-143	No.8	Calcite	Lumpy	−2.7	17.6
HQ-8-98			Vein	−3.0	17.8
HZQ-35	Drusy calcite of carbonate strata			0.50	22.1
HZK-33	Drusy calcite of carbonate strata			1.1	23.5
HZQ-74				−0.80	22.6
HZ-2053-29	Baizuo Fm	Whole		0.35	23.2
HZS-40		rock		0.74	22.8
HZ-X-3				−0.24	23.1

$\delta^{18}O_{SMOW}$ = 1.03086 $\delta^{18}O_{PDB}$ + 30.86 (Friedman and O'Neil, 1977).

respectively).

Rare earth element contents of calcites (especially lumpy calcite) in these deposits are significantly higher than those of the carbonate strata of various ages, but lower than those of non-carbonate strata of various ages and Emeishan basalts in the orefield (Table 3). The chondrite-normalized REE patterns of the carbonate strata and non-carbonate strata show $(La)_N > (Ce)_N > (Pr)_N > (Nd)_N$ with $Eu/Eu^* < 1$, whereas Emeishan basalts display $(La)_N > (Ce)_N > (Pr)_N > (Nd)_N$ with $Eu/Eu^* \approx 1$ (Fig. 8).

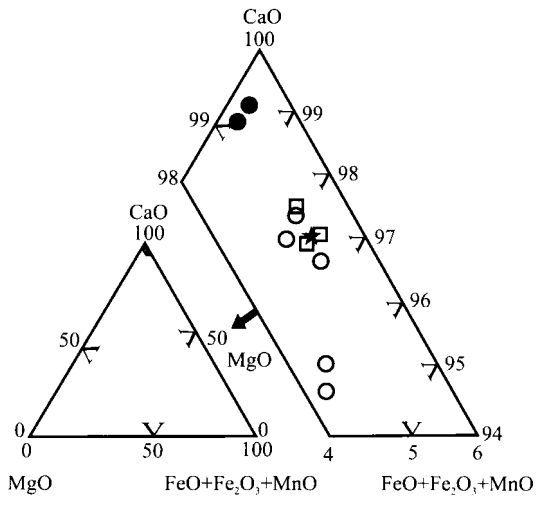

Fig. 6.CaO-MgO-(Fe_2O_3+FeO+MnO) diagram of calcites in the Huize Pb-Zn deposits.
○, lumpy calcite; □, patch calcite; ★, vein calcite; ●, drusy calcite.

4.2 C-O isotope

The C and O isotopic compositions of calcites in the Huize deposits are relatively constant and their $\delta^{13}C_{PDB}$ and $\delta^{18}O_{SMOW}$ values vary from −3.5‰ to −2.1‰ and 16.8‰ to 18.6‰, respectively (Table 2). Moreover, the C and O isotopic compositions of lumpy, patch and vein calcites do not exhibit obvious differences (Table 2). In the diagram of $\delta^{13}C_{PDB}$ vs $\delta^{18}O_{SMOW}$, all of the calcites plot within a small field between the primary mantle and marine carbonate (Fig. 9).

Calcites of the ores have different C and O isotopic compositions from those of drusy calcite in carbonate strata and the Baizuo Formation in the orefield. The $\delta^{13}C_{PDB}$ and $\delta^{18}O_{SMOW}$ values of drusy calcites vary from +0.50‰ to +1.1‰ and 22.1‰ to 23.5‰ and the Baizuo Formation vary from −0.80‰ to +0.74 ‰ and 22.6‰ to 23.2‰, respectively. In Fig. 9, both drusy calcite and the Baizuo Formation are plotted within the field of marine carbonate.

5 Discussion

5.1 Genetic relationship among the three types of calcite

Minerographical observation (Huang et al., 2004b) shows that three types of calcites in the Huize Pb-Zn deposits are the same ore-forming age with different stages and its forming sequence is from lumpy to patch to vein calcites. The major elements of the three types of calcites from the Huize Pb-Zn deposits have no obvious differences, with the exception of Sample Cal-3 and Cal-5 (Table 1 and Fig. 6). In the Tb/Ca vs Tb/La diagram, all samples of calcites plot within the hydrothermal field (Fig. 10). The three types of calcites are similar in C and O isotopic compositions (Table 2, Fig. 9). All of these features indicate that they formed from the same source. As shown in Fig. 11, the three types of calcites from the deposits are distributed horizontally in the Y/Ho vs La/Ho diagram, according to Bau and Dulski (1995), indicating that they formed from the same source.

Although there are some differences in REE geochemistry of the three types of calcites from the deposits, the ranges of ΣREE, LREE/HREE, $(La/Yb)_N$, $(La/Sm)_N$, and $(Gd/Yb)_N$ values of the different type of calcites partially overlap (Table 3). In Fig. 12, there are positive correlations between the Sm/Nd ratios and ΣREE, Y contents and Tb/La ratios but negative correlations between the Sm/Nd ratios and LREE/HREE ratios. Those features can also be seen in the same type of calcites (Fig.

12). It demonstrates that the REE geochemistry of the three types of calcites has a tendency of continuous variations and confirms that they are products of different evolution stages of ore-forming fluids. The content of REE of lumpy calcites (early stage) are higher than those of vein calcites (late stage) (Table 1 and 3). This feature is consistent with the findings of Möller et al. (1984) and Davies et al. (1998) that REE contents of the early crystalline calcite from the carbonate system are relatively higher than those of late calcite.

In addition, the major elements, REE geochemistry and C-O isotopic compositions of the drusy calcite in carbonate strata in the orefield are different from those of gangue calcites. In Fig. 10, the gangue calcite is plotted relatively close to the pegmatitic field, but drusy calcite is near the sedimentary field. In Fig. 11, drusy calcite is distributed outside the field of the gangue calcite, which is distributed horizontally. All of these features show that gangue calcite and drusy calcite in the orefield have different sources.

5.2 Source of ore-forming fluids

There is still much controversy on the source of ore-forming fluids of the Huize Pb-Zn deposits (Liu and Lin, 1999; Zhou et al., 2001; Han et al., 2004; Li et al., 2006). Liu and Lin (1999) and Han et al. (2004) reported that the δD_{H2O} and $\delta^{18}O_{H2O}$ values of fluid inclusions in gangue calcite from these deposits vary from −75‰ to −44‰ and 6.44‰ to 10.1‰, respectively, which are mainly within the respective ranges of the δD_{H2O} (from −90‰ to −50‰) and $\delta^{18}O_{H2O}$ (from 6‰ to 10‰) for magmatic waters, suggesting that the H_2O in the ore-forming fluids are derived predominately from magmas or mantle. Li et al. (2006) reported that the $\delta^{34}S$ values of 46 samples of galena, sphalerite and pyrite in these deposits ranged between 13‰ and 17‰, which are close to those of sulfate (from 14‰ to 18‰) from the carbonate strata with different ages in the orefield (Liu and Lin, 1999), suggesting that the S in the ore-forming fluids mainly came from the sulfate-bearing carbonate strata in the orefield. REE geochemistry and C-O

Table 3 The statistic results of rare earth element (REE) of calcites, strata and Emeishan basalts in the Huize giant Pb-Zn deposits (μg/g)

Name		ΣREE	ΣLREE	ΣHREE	LREE/HREE	Eu/Eu*	Ce/Ce*	(La/Sm)n	(La/Pr)n	(Gd/Yb)n	(La/Yb)n
Lumpy calcite (18)	Range	31.90–357.14	24.11–238.40	2.62–40.45	3.73–17.91	0.33–0.96	1.08–1.25	0.36–1.93	0.35–0.84	2.67–64.90	2.67–131.63
	Average	106.94	77.34	10.46	8.71	0.62	1.18	0.87	0.55	18.43	30.23
Patch calcite (7)	Range	22.60–106.67	18.39–95.92	1.71–7.72	8.22–24.95	1.14–2.04	1.11–1.28	0.59–3.51	0.43–1.21	3.42–50.08	6.86–223.44
	Average	65.16	55.24	4.15	14.98	1.56	1.16	1.63	0.71	13.85	47.13
Vein calcite (3)	Range	23.70–36.24	22.53–34.48	0.60–1.04	30.71–40.70	1.73–2.53	1.00–1.03	4.32–6.24	1.41–1.63	15.75–34.11	137.10–353.01
	Average	31.35	29.65	0.83	36.24	2.17	1.01	5.07	1.51	22.62	209.97
Drusy calcite (4)**	Range	1.90–9.74	0.66–2.93	0.22–1.32	2.22–5.67	0.74–3.71	0.61–1.18		2.11–2.64	1.53–1.84	4.38–6.81
	Average	4.14	1.53	0.52	3.64	1.93	0.85		2.31	1.68	5.85
Dengying Formation (3)	Range	1.91–7.72	0.97–5.42	0.34–0.94	2.85–5.79	0.53–0.70	0.91–1.07	1.34–3.28	1.31–1.85	1.79–2.82	4.80–8.85
	Average	4.54	3.07	0.57	5.03	0.62	1.00	2.48	1.63	2.33	6.82
Qongzhisi Formation	(1)	227.47	176.60	22.67	7.79	0.60	1.01	3.84	1.72	1.33	7.60
Haikou Formation	(1)	102.74	80.38	8.68	9.26	0.48	1.02	6.90	1.98	0.78	8.13
Zaige Formation (4)	Range	10.38–34.46	7.61–25.59	1.20–3.84	5.20–6.67	0.51–0.70	0.78–1.32	2.03–4.02	1.24–2.16	1.23–2.81	5.02–7.79
	Average	20.12	13.86	2.33	5.86	0.61	1.07	2.70	1.64	1.92	6.64
Datang Formation (2)	Range	11.99–15.92	9.20–12.48	1.06–1.33	8.71–9.37	0.68–0.68	1.09–1.17	4.11–4.63	1.81–2.12	1.90–2.15	10.23–11.34
	Average	13.96	10.84	1.19	9.04	0.68	1.13	4.37	1.97	2.02	10.79
Baizuo Formation (6)	Range	3.05–8.97	1.82–6.63	0.32–0.78	3.72–8.45	0.39–0.71	0.67–1.82	1.95–3.48	1.55–2.03	0.94–2.38	4.29–11.22
	Average	4.74	2.95	0.54	5.30	0.56	1.06	3.07	1.84	1.54	6.19
Weining Formation (3)	Range	9.31–40.51	6.92–28.98	1.03–3.86	6.74–7.51	0.43–0.76	1.02–1.15	2.30–5.10	1.21–2.28	1.52–2.33	6.22–11.07
	Average	19.87	14.47	1.99	7.06	0.60	1.07	3.81	1.82	1.87	8.59
Maping Formation (2)	Range	23.11–39.48	15.07–25.21	2.93–4.03	5.15–6.26	0.60–0.67	0.39–0.66	3.13–4.69	1.64–2.14	2.10–2.26	7.63–13.28
	Average	31.30~	20.14	3.48	5.70	0.64	0.52	3.91	1.89	2.18	10.46
Liangshan Formation	(1)	65.75	51.21	5.90	8.68	0.41	1.07	3.77	1.68	1.24	7.66
Qixia-Maokou Formation (3)	Range	0.94–1.90	0.57–0.79	0.11–0.22	2.62–4.99	0.84–1.32	0.35–1.26	2.23–12.06	1.78–3.88	0.71–1.15	5.17–7.49
	Average	1.55	0.65	0.17	4.15	1.12	0.76	7.40	2.62	0.98	6.36
Emeishan Basalts (9)	Range	149.01–325.88	98.10–250.61	22.36–36.14	4.39–7.21	0.86–0.95	0.99–1.04	2.04–2.54	1.28–1.43	1.51–2.46	3.83–8.44
	Average	247.38	183.53	29.50	6.10	0.90	1.03	2.23	1.367	2.13	6.66

** The REE contents of drusy calcite of carbonate strata are for reference only, the figure in brackets is number of samples.

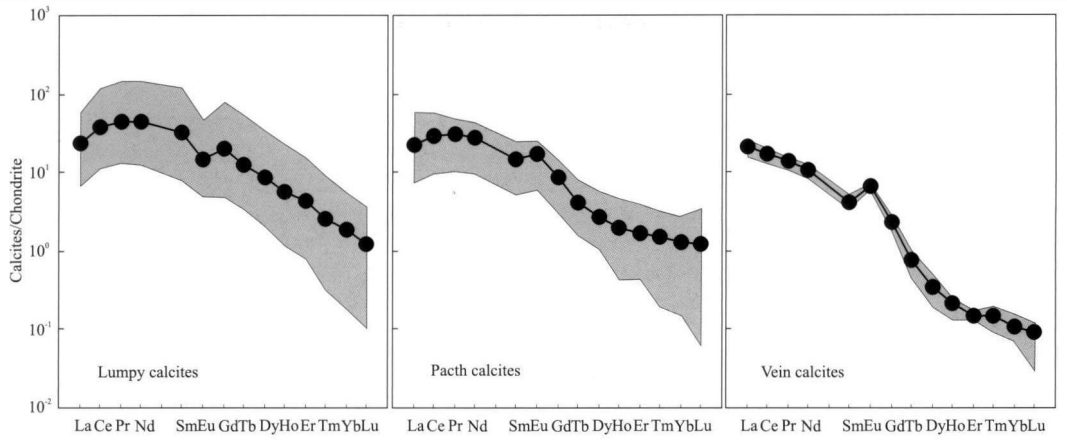

Fig. 7. The chondrite-normalized rare earth element (REE) patterns of calcites in the Huize Pb-Zn deposits. Only displaying the range (shaded area) and average (dotted-line). The chondrite value of REE is taken from Boynton (1984).

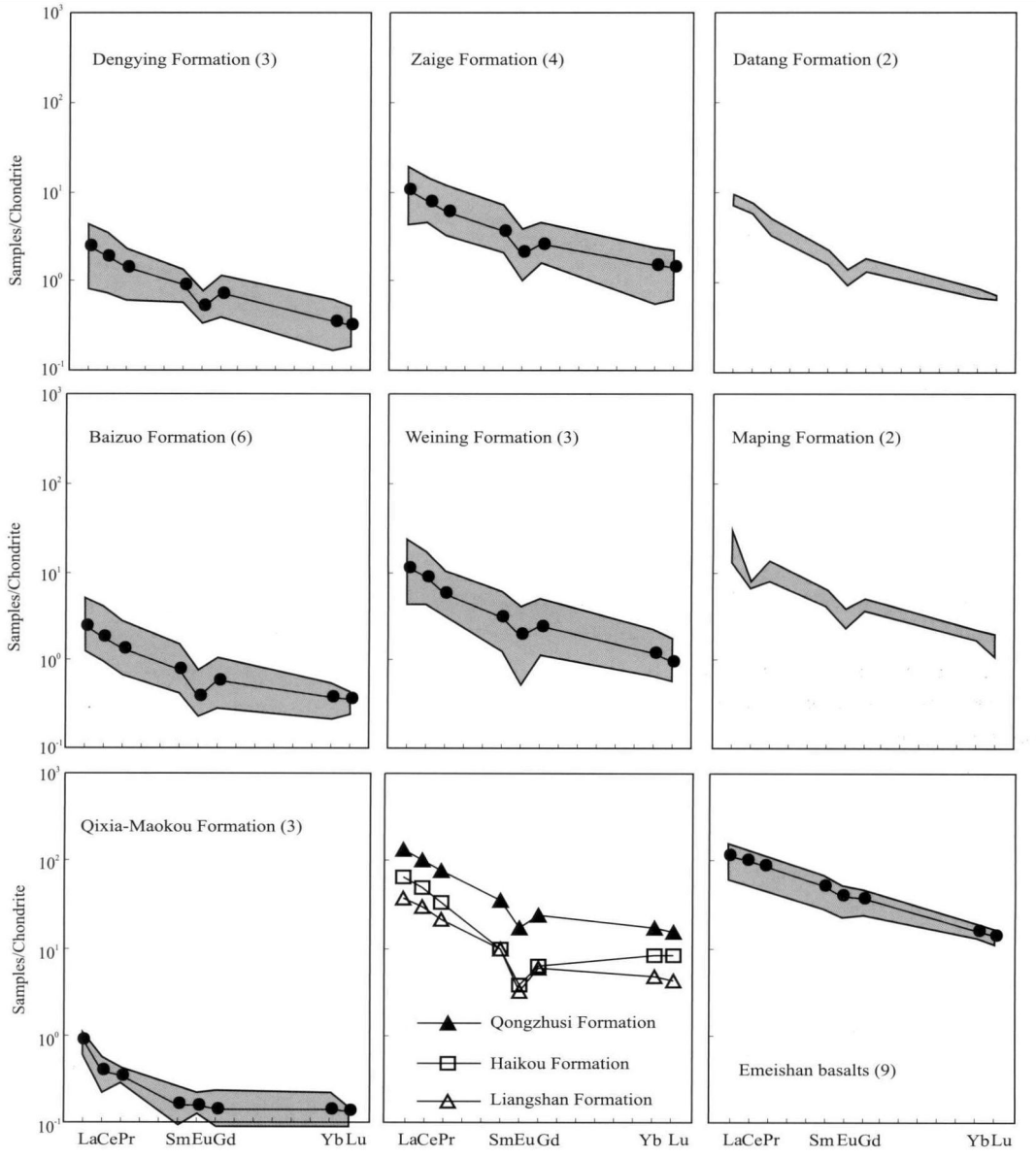

Fig. 8. The chondrite-normalized rare earth element (REE) patterns of strata and Emeishan basalts in the Huize Pb-Zn deposits. The shaded area is a range and the dot-line is an average value. The figure in brackets is the number of samples. The chondrite value of REE is taken from Boynton (1984).

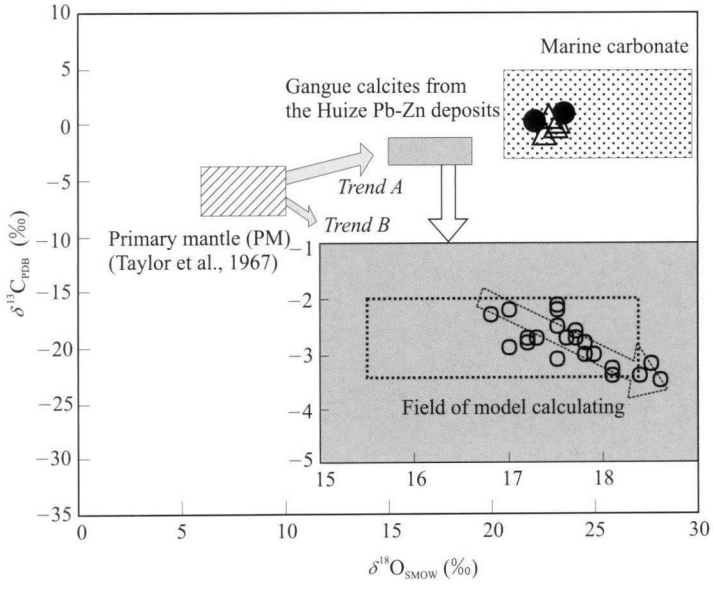

Fig. 9. $\delta^{13}C_{PDB}$ vs $\delta^{18}O_{SMOW}$ diagram of calcite in the Huize Pb-Zn deposits.

○, gangue calcite; ●, drusy calcite; △, the Lower Carboniferous Baizuo Formation. *Trend A* is sedimentary contamination or high temperature fractionation (Demény et al., 1998) and *Trend B* is degassing of magma and /or magmatic fluids (Demény and Haragi, 1996). The dotted rectangle is the range of the $\delta^{13}C_{PDB}$ and $\delta^{18}O_{SMOW}$ values of calculating results by simple binary mixing estimation for the primary mantle (PM) and Baizuo Formation in the orefield. In the processes of calculating, the average of $\delta^{13}C_{PDB}$ and $\delta^{18}O_{SMOW}$ value of Baizuo Formation take 0.01‰ and 22.9‰, respectively (this paper) and those of the PM take –6.7‰ and 8‰, respectively (Demény et al., 1998). The proportion of the Baizuo Formation and PM take from 50% to 70% and 50% to 30%, respectively.

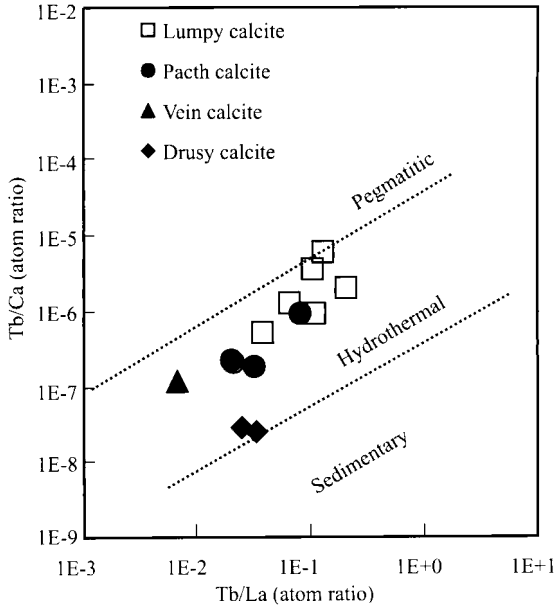

Fig. 10. Tb/Ca *vs* Tb/La diagram of calcite in the Huize Pb-Zn deposits. The primary diagram is taken from Möller et al. (1976).

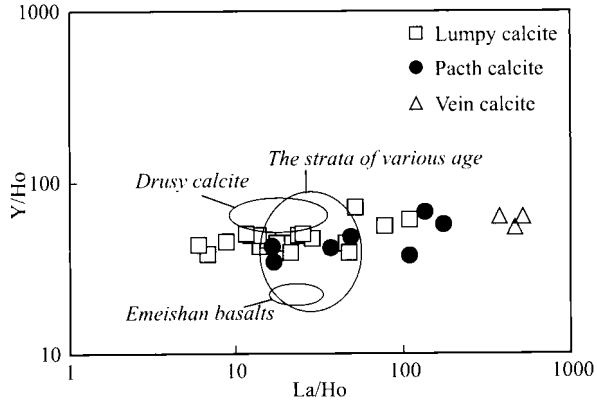

Fig. 11. Y/Ho vs La/Ho diagram of calcite in the Huize Pb-Zn deposits

isotopes reported in this paper suggest that the ore-forming fluids of these deposits are crustal-mantle mixing fluids, as the main evidence is shown as follows:

(1) REE evidence

Because calcite is the main mineral hosting for REE in the Huize Pb-Zn deposits (Han et al., 2000; Li et al., 2007b), its REE geochemistry can represent that of ore-forming fluids. As stated above, since the three types of calcites formed from the same source with different stages, the early ore-forming fluids, which can be represented by lumpy calcite, should be relatively REE-rich.

Rare earth element contents of calcites (especially of early lumpy calcite) in the deposits are significantly higher than those of the carbonate strata of various ages (Table 3). Michard (1989) indicated that relatively REE-rich fluids would not be the product of leaching of the carbonate strata. This conclusion can be supported by REE contents of the drusy calcite in carbonate strata in the orefield, which can be considered as the product of leaching of the carbonate strata, are relatively low (Table 1).Therefore, it is impossible that the ore-forming fluids were provided completely by carbonate strata of various ages in the orefield, since a relatively REE-rich source is required for the ore-forming fluids.

Although REE contents of calcites in the deposits are relatively lower than those of non-carbonate strata of various ages and Emeishan basalts, their chondrite-normalized REE patterns are different from those of the two latter (Figs 7 and 8), and the $(La/Yb)_N$ values are much higher than those of the two latter (Table 3). The experimental results from Ohr et al. (1994) showed that the leachates of argillaceous sediments, which are similar to the non-carbonate strata in this area, have low REE contents (ΣREE< 5 μg/g generally) and $(La/Yb)_N$ values (~2). Therefore, it is impossible that the ore-forming fluids in these deposits were provided completely by the non-carbonate strata and Emeishan basalts. The results also show that relatively REE-rich fluids must be involved in the ore-forming fluids.

Geological and experimental data confirmed that fluids derived from mantle degassing and magmatic degassing are

relatively enriched in REE, especially in LREE (Schrauder et al., 1996; Coltorti et al., 2000; Liu et al., 2004). The ore-forming fluids of the Huize Pb-Zn deposits may have had a mixture of mantle-derived fluids. However, the $(La/Pr)_N$ values of the calcites in the deposits are relatively lower than those of the mantle fluids (Schrauder et al., 1996; Coltorti et al., 2000; Liu et al., 2004). This feature demonstrates that other kinds of fluids with relatively low $(La/Pr)_N$ values were involved in the ore-forming fluids. The experimental result of Möller et al. (1984) and Ohr et al. (1994) showed that the leachates of carbonate and argillaceous sediments, which are similar to the carbonate strata and non-carbonate strata in the orefield, have low REE contents (ΣREE< 5 μg/g) and $(La/Pr)_N$ values (< 1). Therefore, we suggest that these fluids with relatively low $(La/Pr)_N$ values may be the product of leaching of strata of various ages in this area.

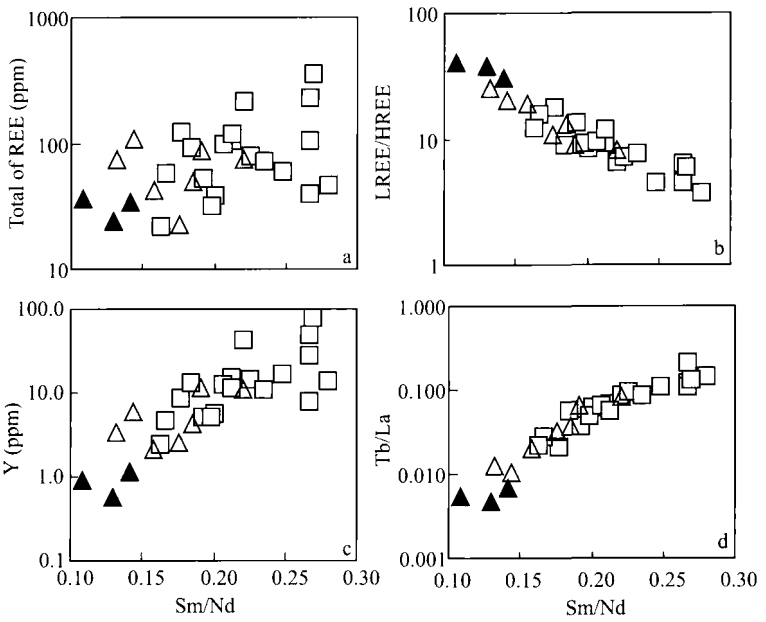

Fig. 12. Sm/Nd vs Σrare earth element (ΣREE) (A), LREE/HREE (B), Y (C) and Tb/La (D) diagram of calcite in the Huize Pb-Zn deposits.
□, lumpy calcite; △, patch calcite; ▲, vein calcite.

(2) C-O isotopic evidence

The C and O isotopic compositions are important for discriminating mantle fluids from crustal fluids. However, abundant analytical data showed that the $\delta^{13}C_{PDB}$ and $\delta^{18}O_{SMOW}$ values of mantle-derived carbonatites are outside the range of the $\delta^{13}C_{PDB}$ (from −8‰ to −4‰) and $\delta^{18}O_{SMOW}$ values (from 6‰ to 10‰) for PM (Taylor et al., 1967; Demény et al., 1998). Previous investigations have proposed sedimentary contamination or high temperature fractionation of primary carbonatite with the the $\delta^{13}C_{PDB}$ and $\delta^{18}O_{SMOW}$ values of PM to explain the origin of carbonatites with Trend A in Fig. 9 (Pineau et al., 1973; Reid and Cooper, 1992; Pearce and Leng, 1996; Horstmann and Verwoerd, 1997; Demény et al., 1998; Andrade et al., 1999; Ray and Ramesh, 1999; Zhang et al., 2009).

In Fig. 9, the C and O isotopic compositions of calcite in the Huize Pb-Zn deposits plot within a small field between PM and marine carbonate (or the Baizuo Formation in the orefield), which can be reasonably explained by the sedimentary contamination or high temperature fractionation of PM. Because the homogenization temperature of fluid inclusions in gangue calcite in the deposits is relatively low (mostly less than 250° C, Han et al., 2004), the high temperature fractionation of primary carbonatite can be excluded. Thus, the C and O isotopic compositions of the calcite may result from of the Baizuo Formation in the orefield contaminated with PM. In Fig. 9, most of the sample plot within the dotted rectangle, with the range of $\delta^{13}C_{PDB}$ and $\delta^{18}O_{SMOW}$ values calculated by simple binary mixing estimation for PM and the Baizuo Formation in the orefield (the calculating processes is shown in the note of Fig. 9). It also confirms that they may be the result of the Baizuo Formation contaminated with PM. That is to say, fluids involved in the mineralization of the Huize Pb-Zn deposits are crustal-mantle mixing fluids.

5.3 The relationship between Emeishan basalts and Pb-Zn mineralization

Because abundant carbonate strata outcrop in the orefield (Figs. 2 and 3), it is possible that the strata provide the crustal compositions for ore-forming fluids. As involvement of the mantle compositions in ore-forming fluids of the Huize Pb-Zn deposits, is it related to the Permian Emeishan basalts magmatism?

The only igneous rocks in the orefield are Permian Emeishan basalts (Fig. 2). There is still controversy on the ore-forming age of the Huize Pb-Zn deposits (including the Sichuan-Yunnan-Guizhou Pb-Zn polymetallic metallogenic province) (Zhang et al., 1988; Liu and Lin, 1999; huang et al., 2001, 2004a, b; Zhou et al., 2001). Based on the statistical results of the age of ore-hosting strata of the Sichuan-Yunnan-Guizhou Pb-Zn polymetallic metallogenic province, Huang et al. (2001) suggested that the ore-forming age of this area is close to the formation age of the Permian Emeishan basalts. Li et al. (2007b) reported that the Sm-Nd age of gangue calcite from orebodies no. 6 and no. 1 in the Huize Pb-Zn deposits is 225±9.9 Ma and 228±16 Ma, respectively. Although these

ages are less than the formation age of the Permian Emeishan basalts (c.260 Ma; Boven et al., 2002; Lo et al., 2002; Zhou et al., 2002; Ali et al., 2004; Fan et al., 2008), lots of investigations showed that it is a general phenomenon of the existence of the time difference between magmatism and mineralization, and the maximum can reach up to 60 Ma (Halliday, 1980; Snee et al, 1988; Chesley et al., 1991; Leach et al., 2001). Thus, the ore-forming age of the deposits provide evidence for the involvement of mantle-derived fluids, which are related to Permian Emeishan basalts magmatism.

Previous investigations have shown that the Emeishan basalts are the product of mantle plume activity (Chung and Jahn, 1995; Chung et al., 1998; Song et al., 2001; Xu et al., 2001, 2004; Ali et al., 2005). Liu et al. (2004) listed geological evidence to indicate that the fluids, which formed from the degassing that accompanied the magmatism of the mantle plume, were involved in the mineralization. Demény and Harangi (1996) suggest that the carbonatites with Trend B in Fig. 9 are the product of degassing of magma and/or magmatic fluids. In Fig. 9, the C and O isotopes of the calcites in the deposits also exhibit the feature of Trend B (i.e. negative correlation between the $\delta^{13}C_{PDB}$ and $\delta^{18}O_{SMOW}$ values), indicating that calcite was influenced by degassing of magma and/or magmatic fluids. Therefore, we propose that the fluids that formed from the degassing of magma and/or magmatic fluids that accompanied the Permian Emeishan basalts magmatism were involved in the mineralization of the Huize Pb-Zn deposits (including the Sichuan-Yunnan- Guizhou Pb-Zn polymetallic metallogenic province).

5.4 The evolution of ore-forming fluids

The REE features of calcites in the Huize Pb-Zn deposits have recorded information about the processes of evolution of the ore-forming fluid. From lumpy to patch to vein calcites, corresponding to the mineralization from early to late, REE variation features are described as follows: (1) REE contents tend to decrease steadily; (2) ratios of Sm/Nd and Tb/La show a tendency of regular variations; and (3) Eu/Eu^* values tend to rise progressively. For the REE contents of ore-forming fluids decreasing steadily, it implies that almost no more relatively REE-rich fluids were involved in mineralization in this area. Regular variations of Sm/Nd and Tb/La seem to be related to the variation of calcite lattice and the physicochemical properties of the ore-forming fluids, that is, dependence on partitioning coefficient of REE between calcite and CO_2-bearing fluid Eu is usually present in the form of Eu^{3+}, but under relatively reducing conditions, part of Eu will be converted to Eu^{2+} and then separated from the other REEs (Brookins, 1989; Barbin et al., 1996; Zhang et al., 2008). As the Eu/Eu^* values of calcite crystallized under relatively reducing conditions are lower than those of calcite formed under relatively oxidizing conditions, it can be deduced that the ore-forming environment in the deposits once experienced a changing process from relatively reducing to oxidizing.

From lumpy to patch to vein calcites, although there exists the variation of REE geochemistry, the C and O isotopic compositions have no obvious difference. This feature shows that almost no more crust or mantle fluids were involved in the evolution of ore-forming fluids in the processes of mineralization. That is to say, the ore-forming fluids in these deposits were homogenized before mineralization. This conclusion was supported by the following evidence.

(1) Li et al. (2006) reported that the S isotopic compositions of the ore mineral (such as galena, sphalerite and pyrite) from various orebodies in the Huize deposits have no obvious differences, and have $\delta^{34}S_{pyrite}$ (from 14.92% to 16.42‰; 17 samples) > $\delta^{34}S_{sphalerite}$ (from 13.36% to 16.02‰; 21 samples) > $\delta^{34}S_{galena}$ (from 11.25% to 14.49‰; 8 samples). These features show that the S in the ore-forming fluids had been homogenized and equilibrated before mineralization.

(2) From Zhou et al. (2001), Han et al. (2007) and our unpublished data, the Pb isotopic compositions of ore mineral (such as galena, sphalerite and pyrite) from various orebodies in the deposits have also no obvious difference, and their $^{206}Pb/^{204}Pb$, $^{207}Pb/^{204}Pb$, $^{208}Pb/^{204}Pb$ range from 18.461 to 18.514, 15.664 to 15.754, and 38.729 to 39.009, respectively. It suggests that the Pb isotope in the ore-forming fluids had been homogenized before mineralization.

(3) The geological characteristics of the deposits, such as the different primary orebody composed by galena, sphalerite, pyrite, and calcite, the presence of distinct boundaries between orebody and wall rock, and simple whole-rock alteration represented by dolomitization and pyritization, also demonstrate that the deposits are the product of single-event mineralization of the homogeneous ore-forming fluids.

6 Conclusions

Calcite, which formed throughout the mineralization processes, is the only gangue mineral in the primary ores of the world-class Huize Pb-Zn deposits and can be classified into three types, namely lumpy, patch and vein calcites in accordance with their occurrence. Minerographical observation shows that three types of calcites are the same ore-forming age with different stages, and its forming sequence is from lumpy to patch to vein calcites. Although

there are some differences in REE geochemistry among three types of gangue calcite, the REE geochemistries of the different (or the same) type of calcites show a tendency of continuous variation. The different types of gangue calcites are similar in the C and O isotopic compositions, suggesting that the three types of calcites are the product from the same source but at different evolution stage of ore -forming fluids.

Rare earth element contents of calcites (especially of early lumpy calcite) are significantly higher than those of the carbonate strata of various ages, and lower than those of the non-carbonate strata of various ages and the Permian Emeishan basalts in the orefield. The C and O isotopic compositions of the three types of calcites plot within a small field between primary mantle (PM) and marine carbonate. We consider here that the ore-forming fluids of these deposits are crustal-mantle mixing fluids, in which the mantle fluid component might be formed from degassing of mantle or mantle-derived magma accompanying magmatism of Permian Emeishan basalt, and crustal fluids were mainly provided by carbonate strata in the orefield.

From lumpy to patch to vein calcites, REE contents tend to decrease with increasing Eu/Eu*, indicating that the REE contents of ore-forming fluids tend to decrease in the processes of mineralization and the ore-forming environment varied from relatively reducing to oxidizing. In addition, thinking of similar mineral associations in these deposits, and contact relations between orebody and wall rock, and development of alteration in whole rocks, and no obvious differences in C-O isotopes of calcites, and S, Pb isotopes in ore minerals, all of these evidences declare that the ore-forming fluids of the deposits were homogenized before mineralization.

Acknowledgements

This research project was granted jointly by National Basic Research Program of China (973 Program) (2007CB411402), the Knowledge innovation project of Chinese Academy of Sciences (KZCX2-YW-Q04-05, KZCX2-YW-111-03) and the National Natural Science Foundation of China (No. 40573036). We thank Liang Oi in Institute of Geochemistry, Chinese Academy of Sciences for measuring REE contents. We further thank Prof. Congqiang Liu and Prof. Ruizhong Hu in Institute of Geochemistry, Chinese Academy of Sciences whose reviews helped improve this manuscript.

Manuscript received Sept. 20, 2008
accepted Jan. 5, 2009
edited by Fei Hongcai

References

Ali, J.R., Lo, C.H., Thompson, G.M., and Song, X.Y., 2004. Emeishan Basalt Ar–Ar overprint ages define several tectonic events that affected the western Yangtze Platform in the Mesozoic and Cenozoic. *Journal of Asian Earth Sciences*, 23: 163–178.

Ali, J.R., Thompson, G.M., Zhou, M.F., and Song, X.Y., 2005. Emeishan large igneous province, SW China. *Lithos*, 79: 475–489.

Alvin, M.P., Dunphy, J.M., and Groves, D.I., 2004. Nature and genesis of a carbonatite-associated fluorite deposit at Speewah, East Kimberley region, Western Australia. *Mineralogy and Petrolgy*, 80: 127–153.

Andrade, F.R.D., Möller, P., Lüders, V., Dulski P., and Gilg, H.A., 1999. Hydrothermal rare earth elements mineralization in the Barra do Itapirapuã carbonatite, southern Brazil: behaviour of selected trace elements and stable isotopes (C, O). *Chemical Geology*, 155: 91–113.

Barbin, V., Jouart, J.P., and D'Almeida, T., 1996. Cathodoluminescence and laser-excited luminescence spectroscopy of Eu^{3+} and Eu^{2+} in synthetic CaF_2: a comparative study. *Chemical Geology*, 130: 77–86.

Bau, M., and Dulski, P., 1995. Comparative study of yttrium and rare-earth element behaviours in fluorine-rich hydrothermal fluids. *Contributions to Mineralogy and Petrology*, 119: 213–223.

Bau, M., Romer, R.L., Lüders, V., and Dulski, P., 2003. Tracing element sources of hydrothermal mineral deposits: REE and Y distribution and Sr-Nd-Pb isotopes in fluorite from MVT deposits in the Pennine Orefield, England. *Mineralium Deposita*, 38: 992–1008.

Boven, A., Pasteels, P., Punzalan, L.E., Liu, J., Luo, X., Zhang, W., Guo, Z., and Hertogen, J., 2002. $^{40}Ar/^{39}Ar$ geochronological constraints on the age and evolution of the Permo-Triassic Emeishan Volcanic Province, Southwest China. *Journal of Asian Earth Sciences*, 20: 157–175.

Boynton, W.V., 1984. Cosmochemistry of the rare earth elements: meteorite studies. *Dev. Geochem.* 2, 63–114.

Brookins, D.G., 1989. Aqueous geochemistry of rare earth elements. *Reviews in Mineralogy*, 21: 201–225.

Brugger, J., Lahaye, Y., Costa, S., Lambert, D., and Bateman, R., 2000. Inhomogeneous distribution of REE in scheelite and dynamics of Archaean hydrothermal systems (Mt. Charlotte and Drysdale gold deposits, Western Australia). *Contributions to Mineralogy and Petrology*, 139: 251–264.

Bühn, B., Schneider, J., Dulski, P., and Rankin, A.H., 2003. Fluid-rock interaction during progressive migration of carbonatitic fluids, derived from small-scale trace element and Sr, Pb isotope distribution in hydrothermal fluorite. *Geochimica et Cosmochimica Acta*, 67: 4577– 4595.

Chen Jin, Han Runsheng, Gao Derong and Zhao Deshun, 2001. Geogolical characteristics of the Huize Pb-Zn deposit, Yunnan and model of ore-prospecting method. *Geology geochemistry*, 29(3): 124–129 (in Chinese with English abstract).

Chung, S.L., and Jahn, B.M., 1995. Plume-lithosphere interaction in generation of the Emeishan flood basalts at the Permian-Triassic boundary. *Geology*, 23: 889–892.

Chung, S.L., Jahn, B.M., Wu, G.Y., Lo, C.H., and Cong, B.L., 1998. The Emeishan flood basalt in SW China: a mantle plume initiation model and its connection with continental break-up and mass extinction at the Permian-Triassic

boundary. In: M.F.J. Flower, S.L. Chung, C.H. Lo and T.Y. Lee, Editors, *Mantle Dynamics and Plate Interaction in East AsiaAGU Geodyn.* Ser. vol. 27, AGU, Washington, D.C. 47–58.

Coltorti, M., Beccaluva, L., Bonadiman, C., Salvini, L., and Siena, F., 2000. Glasses in mantle xenoliths as geochemical indicators of metasomatic agents. *Earth and Planetary Science Letters*, 183: 303–320.

Davies, J.F., Prevec, S.A., Whitehead, R.E., and Jackson, S.E., 1998. Variations in REE and Sr-isotope chemistry of carbonate gangue, Castellanos Zn-Pb deposit, Cuba. *Chemical Geology*, 144: 99–119.

Deines, P., 1989. Stable isotope variations in carbonatites. In: Bell, K. (ed.), *Carbonatites: Genesis and evolution*. Unwin Hyman, London, Boston, Sydney, Wellington. 301–359.

Demény, A., Ahijado, A., Casillas R., and Vennemann, T.W., 1998. Crustal contamination and fluid/rock interaction in the carbonatites of Fuerteventura (Canary Islands, Spain): a C, O, H isotope study. *Lithos*, 44: 101–115.

Demény, A., and Harangi, Sz., 1996. Stable isotope studies on carbonate formations in alkaline basalt and lamprophyre series: evolution of magmatic fluids and magma-sediment interactions. *Lithos*, 37: 335–349.

Fan, W.M., Zhang, C.H., Wang, Y.J., Guo, F., Peng, T. P., 2008. Geochronology and geochemistry of Permian basalts in western Guangxi Province, Southwest China: Evidence for plume-lithosphere interaction. *Lithos*, 102: 218–236.

Ghaderi, M., Palin, M.J., Sylvester, P.J., and Campbell, I.H., 1999. Rare earth element systematics in scheelites from hydrothermal gold deposits in the Kalgoorlie-Norseman region, Western Australia. *Economic Geology*, 94: 423–438.

Han Runsheng, Liu Congqiang, Huang Zhilong, Chen Jin, Ma Deyun, Lei Li and Ma Gengsheng, 2007. Geological features and origin of the Huize carbonate-hosted Zn–Pb–(Ag) District, Yunnan, South China. *Ore Geology Reviews*, 31: 360–383.

Han Runsheng, Liu Congqiang, Huang Zhilong, Ma Deyun, Li Yuan, Hu Bin, Ma Gengsheng and Lei Li, 2004. Fluid inclusions of calcite and sources of ore-forming fluids in the Huize Zn-Pb-(Ag-Ge) district, Yunnan, China. *Acta Geologica Sinica* (English Edition), 78: 583–591.

Han Runsheng, Liu Congqiang, Huang Zhilong, Ma Deyun and Li Yuan, 2000. Features of structural control of minerals and fault structural rock rare earth element for Huize Pb-Zn Deposit, Yunnan. *Journal of Mineralogy and Petrology*, 21 (4): 11–18 (in Chinese with English abstract).

Hecht, L., Freiberger, R., and Gilg, T.A., Grundmann, G., Kostitsyn, Y.A., 1999. Rare earth element and isotope (C, O, Sr) characteristics of hydrothermal carbonates: genetic implications for dolomite-hosted talc mineralization at Göpfersgrün (Fichtelgebirge, Germany). *Chemical Geology*, 155: 115–130.

Hoernle, K., Tilton, G., Le Bas, M.J., and Duggen, S., Garbe-Schonberg, D., 2002. Geochemistry of oceanic carbonatites compared with continental carbonatites: mantle recycling of oceanic crustal carbonate. *Contributions to Mineralogy and Petrology*, 142: 520–542.

Horstmann, U.E., and Verwoerd, W.J., 1997. Carbon and oxygen isotope variations in southern African carbonatites. *Journal of African Earth Sciences*, 25: 115–136.

Hu Ruizhong, Tao Yan, Zhong Hong, Huang Zhilong and Zhang Zhengwei, 2005. Mineralization systems of a mantle plume: A case study from the Emeishan igneous province, southwest China. *Earth Science Frontiers*, 12: 42–54. (in Chinese with English abstract).

Huang Zhilong, Xu Cheng, McCaig A, Liu Congqiang, Wu Jing, Xu Deru, Li Wenbo, Guan Tao and Xiao Huayun, 2007. REE Geochemistry of fluprite from the Maoniuping REE deposit, Sichuan Province, China: implications for the source of ore-forming fluids. *Acta Geological Sinica* (English Edition), 81: 622–636

Huang Zhilong, Li Wenbo, Zhang Zhenliang, Han Runsheng and Chen Jin, 2004. Severl problems involved in genetic studies on the Huize super-large Pb-Zn deposit, Yunnan Province. *Acta Mineralogical Sinica*, 24: 105–111 (in Chinese with English abstract).

Huang Zhilong, Chen Jin, Liu Congqiang, Han Runsheng, Li Wenbo, Zhao Deshun, Gao Derong and Feng Zhihong, 2001. Preliminary the relationship between Emeishan basalts and Pb-Zn mineralization: As examplified by the Huize Pb-Zn deposits, Yunnan Province, China. *Acta Mineralogical Sinica*, 21, 691–697 (in Chinese with English abstract).

Keller, J., and Hoefs, J., 1995. Stable isotope characteristics of recent natrocarbonatites from Oldoinyo Lengai. In: Bell, K., and Keller, J. (eds.), *Carbonatite Volcanism: Oldoinyo Lengai and the Petrogenesis of Natrocarbonatites*. Springer, Berlin. 113–123.

Li Wenbo, Huang Zhilong and Qi Liang, 2007a. REE geochemistry of sulfides from the Huize Zn-Pb ore field, Yunnan Province: implication for the sources or ore-forming metals. *Acta Geologica Sinca* (English Edition), 81(3): 442–449

Li Wenbo, Huang Zhilong and Yin Mudan, 2007b. Dating of the giant Huize Zn-Pb ore field of Yunnan Province, Southwest China: constraints from the Sm-Ndsystem in hydrothermal calcite. *Resource Geology*, 57: 90–97.

Li Xiaobiao, Huang Zhilong, Li Wenbo, Zhang Zhenliang and Yan Zaifei, 2006. Sulfur isotopic compositions of the Huize super-large Pb-Zn deposit, Yunnan province, China: Implications for the source of sulfur in the ore-forming fluids. *Journal of Geochemical Exploration*, 89: 227–230.

Liu Congqiang, Huang Zhilong, Xu Cheng, Zhang Hongxiandg, Su Gengli, Li Heping and Qi Liang, 2004. *Geofluids in the Earth's Mantle and its Role in Mineralization: A Case Study the Mianning REE Deposit, Sichuan Province, China*. Beijing: Geological Publishing House (in Chinese).

Liu Hechang and Lin Wenda, 1999. *Study on the law of Pb-Zn-Ag Ore Dposit in Northeast Yunnan, China*. Kunmaing: Yunnan University Press (in Chinese).

Lo, C.H., Chung, S.L., Lee, T.Y., and Wu, G.Y., 2002. Age of the Emeishan flood magmatism and relations to Permian–Triassic boundary events. *Earth and Planetary Science Letters*, 198: 449–458.

Lottermoser, B.G., 1992. Rare earth elements and hydrothermal ore formation processes. *Ore Geology Reviews*, 7: 25–41.

Michard, A., 1989. Rare earth element systematics in hydrothermal fluids. *Geochimica et Cosmochimica Acta*, 53: 745–750.

Möller, P., Morteani, G., and Dulski, P., 1984. The origin of the calcites from Pb-Zn veins in the Harz Mountains, Federal Republic of Germany. *Chemical Geology*, 45: 91–112.

Möller, P., Parekh, P.P., and Schneider, H.J., 1976. The

application of Tb/Ca—Tb/La abundance ratios to problems of fluorite genesis. *Mineralium Deposita*, 11: 111–116.

Monecke, T., Monecke, J., Mönch, W., and Kempe, U., 2000. Mathematical analysis of rare earth element patterns of fluorites from the Ehrenfriedersdorf tin deposit, Germany: evidence for a hydrothermal mixing process of lanthanides from two different sources. *Mineralogy and Petrolgy*, 70: 235–256.

Ohr, M., Halliday, A.N., and Peacor, D.R., 1994. Mobility and fractionation of rare earth element in argillaceous sediments: implications for dating diagenesis and low-grade metamorphism. *Geochimica et Cosmochimica Acta*, 58: 289–312.

Pearce, N.J.G., and Leng, M.J., 1996. The origin of carbonatites and related rocks from the Igaliko Dyke Swarm, Gardar Province, South Greenland: field, geochemical and C-O-Sr-Nd isotope evidence. *Lithos*, 39: 21–40.

Pineau, F., Javoy, M., and Allegre, C.J., 1973. Etude systématique des isotopes de l'oxygéne, du carbone et du strontium dans les carbonatites. *Geochimica et Cosmochimica Acta*, 37: 2363–2377.

Qi Liang, Hu Jin and Gregoire, D.C., 2000. Determination of trace elements in granites by inductively coupled plasma mass spectrometry. *Talanta*, 51: 507–513.

Ray, J.S., and Ramesh, R., 1999. Evolution of carbonatite complexes of the Deccan flood basalt province: stable carbon and oxygen isotopic constraints. *Journal of Geophysical Research*, 104(B12): 29471–29483.

Reid, D.L., and Cooper, A.F., 1992. Oxygen and carbon isotope patterns in the Dicker Willem carbonatite complex, southern Namibia. *Chemical Geology*, 94: 293–305.

Ruberti, E., Castorina, F., Censi, P., Comin-Chiaramonti, P., Gomes, C.B., Antonini, P., Andrade, F.R.D., 2002. The geochemistry of the Barra do Itapirapua carbonatite (Ponta Grossa Arch, Brazil): a multiple stockwork. *Journal of South American Earth Sciences*, 15: 215–228.

Schrauder, M., Koeberl, C., and Navon, O., 1996. Trace element analyses of fluid-bearing diamonds from Jwaneng, Botswana. *Geochimica et Cosmochimica Acta*, 60: 4711–4724.

Schwinn, G., and Markl, G., 2005. REE systematics in hydrothermal fluorite. *Chemical Geology*, 216: 225–248.

Song, X.Y., Zhou, M.F., Hou, Z.Q., Cao, Z.M., Wang, Y.L., and Li, Y.G., 2001. Geochemical Constraints on the Mantle Source of the Upper Permian Emeishan Continental Flood Basalts, Southwestern China. *International Geology Review*, 43: 213–225.

Subías, I., and Fernández-Nieto, C., 1995. Hydrothermal events in the Valle de Tena (Spanish Western Pyrenees) as evidenced by fluid inclusions and trace-element distribution from fluorite deposits. *Chemical Geology*, 124: 267–282.

Taylor, Jr., H.P., Frechen, J., and Degens, E.T., 1967. Oxygen and carbon isotope studies of carbonatites from the Laacher See District, West Germany and the Alno District Sweden. *Geochimica et Cosmochimica Acta*, 31: 407–430.

Whitney, P.R., and Olmsted, J.F., 1998. Rare earth element metasomatism in hydrothermal systems: the Willsboro-Lewis wollastonite ores, New York, USA. *Geochimica et Cosmochimica Acta*, 62: 2965–2977.

Xu Cheng, Huang Zhilong, Liu Congqiang, Qi Liang, Xiao Huayun and Li Wenbo, 2003. The geochemistry of carbonatites in Maoniuping REE deposits, Sichuan Province, China. *Science in China* (D), 46: 246–256.

Xu, Y.G., Chung, S.L., Jahn, B.M., and Wu, G.Y., 2001. Petrologic and geochemical constraints on the petrogenesis of Permian-Triassic Emeishan flood basalts in southwestern China. *Lithos*, 58: 145–168.

Xu, Y.G., He, B., Chung, S.L., Menzies, M.A., and Frey, F.A., 2004. The geologic, geochemical and geophysical consequences of plume involvement in the Emeishan flood basalt province. *Geology*, 30: 917–920.

Zhang Chengjun, Steffen Mischke, Zheng Mianping, Alexander Prokopenko, Guo Fangqin and Feng Zhaodong, 2009. Carbon and Oxygen Isotopic Composition of Surface-Sediment Carbonate in Bosten Lake (Xinjiang, China) and its Controlling Factors. *Acta Geologica Sinica* (English edition), 83: 386–395.

Zhang Xuefeng, Hu Wenxuan, Jin Zhijun, Zhang Juntao, Qian Yixiong, Zhu Jingquan, Zhu Dongya, Wang Xiaolin and Xie Xiaomin, 2008. REE Compositions of Lower Ordovician Dolomites in Central and North Tarim Basin, NW China: A Potential REE Proxy for Ancient Seawater. *Acta Geologica Sinica* (English edition), 82: 610–621.

Zhang Yunxiang, Luo Yaonan, and Yang Congxi, 1988. *The Panzhihua-Xichang Rift in China*. Beijing: Geological Publishing House (in Chinese).

Zhou, C.X., Wei, C.S., and Guo, J.Y., 2001. The source of metals in the Qilingchang Pb-Zn deposit, Northeastern Yunnan, China: Pb-Sr isotope constraints. *Economic Geology*, 96: 583–598.

Zhou, M.F., Malpas, J., Song, X.Y., Robinson, P.T., Sun, M., Kennedy, A.K., Lesher, C.M., and Keays, R.R., 2002. A temporal link between the Emeishan large igneous province (SW China) and the end-Guadalupian mass extinction. *Earth and Planetary Science Letters*, 196: 113–122.